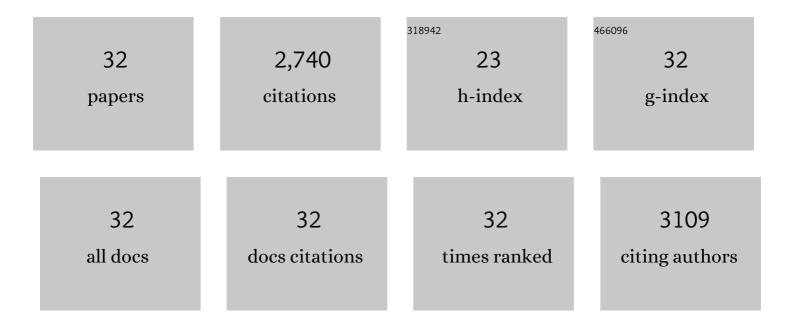
## **Bo Sheng**

List of Publications by Year in descending order

Source: https://exaly.com/author-pdf/4691301/publications.pdf Version: 2024-02-01



RO SHENC

#	Article	IF	CITATIONS
1	Non-radical pathway dominated by singlet oxygen under high salinity condition towards efficient degradation of organic pollutants and inhibition of AOX formation. Separation and Purification Technology, 2022, 291, 120921.	3.9	9
2	Performance of UV/acetylacetone process for saline dye wastewater treatment: Kinetics and mechanism. Journal of Hazardous Materials, 2021, 406, 124774.	6.5	17
3	Cu2+/Cu+ cycle promoted PMS decomposition with the assistance of Mo for the degradation of organic pollutant. Journal of Hazardous Materials, 2021, 411, 125050.	6.5	105
4	Resistance of alkyl chloride on chloramphenicol to oxidative degradation by sulfate radicals: Kinetics and mechanism. Chemical Engineering Journal, 2021, 415, 129041.	6.6	21
5	Resolving the kinetic and intrinsic constraints of heat-activated peroxydisulfate oxidation of iopromide in aqueous solution. Journal of Hazardous Materials, 2020, 384, 121281.	6.5	3
6	Transformation of endogenic and exogenic Cl/Br in peroxymonosulfate-based processes: The importance of position of Cl/Br attached to the phenolic ring. Chemical Engineering Journal, 2020, 381, 122634.	6.6	26
7	Is addition of reductive metals (Mo, W) a panacea for accelerating transition metals-mediated peroxymonosulfate activation?. Journal of Hazardous Materials, 2020, 386, 121877.	6.5	44
8	Hierarchical MnO2 nanoflowers blooming on 3D nickel foam: A novel micro-macro catalyst for peroxymonosulfate activation. Journal of Colloid and Interface Science, 2020, 571, 142-154.	5.0	94
9	Accelerated oxidation of 2,4,6-trichlorophenol in Cu(II)/H2O2/Cl- system: A unique "halotolerant― Fenton-like process?. Environment International, 2019, 132, 105128.	4.8	22
10	Ultrahigh-flux (>190,000†L·mâ^'2hâ^'1) separation of oil and water by a robust and durable Cu(OH)2 nanoneedles mesh with inverse wettability. Journal of Colloid and Interface Science, 2019, 555, 569-582.	5.0	18
11	Pivotal roles of MoS2 in boosting catalytic degradation of aqueous organic pollutants by Fe(II)/PMS. Chemical Engineering Journal, 2019, 375, 121989.	6.6	192
12	An often-overestimated adverse effect of halides in heat/persulfate-based degradation of wastewater contaminants. Environment International, 2019, 130, 104918.	4.8	36
13	Chlorine incorporation into dye degradation by-product (coumarin) in UV/peroxymonosulfate process: A negative case of end-of-pipe treatment. Chemosphere, 2019, 229, 374-382.	4.2	25
14	On peroxymonosulfate-based treatment of saline wastewater: when phosphate and chloride co-exist. RSC Advances, 2018, 8, 13865-13870.	1.7	26
15	Nanostructured Co3O4 grown on nickel foam: An efficient and readily recyclable 3D catalyst for heterogeneous peroxymonosulfate activation. Chemosphere, 2018, 198, 204-215.	4.2	109
16	Co3O4 nanocrystals/3D nitrogen-doped graphene aerogel: A synergistic hybrid for peroxymonosulfate activation toward the degradation of organic pollutants. Chemosphere, 2018, 210, 877-888.	4.2	81
17	Deciphering the degradation/chlorination mechanisms of maleic acid in the Fe(II)/peroxymonosulfate process: An often overlooked effect of chloride. Water Research, 2018, 145, 453-463.	5.3	73
18	Enhancement of adhesion, mechanical strength and anti-corrosion by multilayer superhydrophobic coating embedded electroactive PANI/CNF nanocomposite. Journal of Polymer Research, 2018, 25, 1.	1.2	26

BO SHENG

#	Article	IF	CITATIONS
19	Facile fabrication approach for a novel multifunctional superamphiphobic coating based on chemically grafted montmorillonite/Al2O3-polydimethylsiloxane binary nanocomposite. Journal of Polymer Research, 2017, 24, 1.	1.2	19
20	Durable Selfâ€Healing Superhydrophobic Coating with Biomimic "Chloroplast―Analogous Structure. Advanced Materials Interfaces, 2016, 3, 1600040.	1.9	23
21	Superamphiphobic and Electroactive Nanocomposite toward Self-Cleaning, Antiwear, and Anticorrosion Coatings. ACS Applied Materials & Interfaces, 2016, 8, 12481-12493.	4.0	145
22	Toward Efficient Demulsification of Produced Water in Oilfields: Solar STEP Directional Degradation of Polymer on Interfacial Film of Emulsions. Energy & amp; Fuels, 2016, 30, 9686-9692.	2.5	16
23	One-step fabrication of a nickel foam-based superhydrophobic and superoleophilic box for continuous oil–water separation. Journal of Materials Science, 2015, 50, 4707-4716.	1.7	48
24	Superhydrophobic polyaniline hollow spheres with mesoporous brain-like convex-fold shell textures. Journal of Materials Chemistry A, 2015, 3, 19299-19303.	5.2	28
25	A novel carbon nanotubes reinforced superhydrophobic and superoleophilic polyurethane sponge for selective oil–water separation through a chemical fabrication. Journal of Materials Chemistry A, 2015, 3, 266-273.	5.2	348
26	Probing the radical chemistry in UV/persulfate-based saline wastewater treatment: Kinetics modeling and byproducts identification. Chemosphere, 2014, 109, 106-112.	4.2	91
27	Sulfate radical-induced degradation of 2,4,6-trichlorophenol: A de novo formation of chlorinated compounds. Chemical Engineering Journal, 2013, 217, 169-173.	6.6	97
28	Concentration profiles of chlorine radicals and their significances in •OH-induced dye degradation: Kinetic modeling and reaction pathways. Chemical Engineering Journal, 2012, 209, 38-45.	6.6	60
29	Photocatalytic degradation and chlorination of azo dye in saline wastewater: Kinetics and AOX formation. Chemical Engineering Journal, 2012, 192, 171-178.	6.6	123
30	Effects of chloride ion on degradation of Acid Orange 7 by sulfate radical-based advanced oxidation process: Implications for formation of chlorinated aromatic compounds. Journal of Hazardous Materials, 2011, 196, 173-179.	6.5	502
31	Degradation of reactive dyes by contact glow discharge electrolysis in the presence of Clâ^' ions: Kinetics and AOX formation. Electrochimica Acta, 2011, 58, 364-371.	2.6	40
32	Effects of chloride ions on bleaching of azo dyes by Co2+/oxone regent: Kinetic analysis. Journal of Hazardous Materials, 2011, 190, 1083-1087.	6.5	273